KfK 4584
Mai 1989

Nuclear Structure Effects in Elastic $^{12}C + ^{12}C$ Scattering

S. Galachmatova, E. Romanovsky, A. Shirokova,
K. V. Shitikova, H. J. Gils, H. Rebel
Institut für Kernphysik

Kernforschungszentrum Karlsruhe

KERNFORSCHUNGSZENTRUM KARLSRUHE

Institut für Kernphysik

KfK 4584

Nuclear Structure Effects in Elastic $^{12}C + ^{12}C$ Scattering

S. Galachmatova*, E. Romanovsky*, A. Shirokova*,
K.V. Shitikova*, H.J. Gils and H. Rebel

Kernforschungszentrum Karlsruhe GmbH, Karlsruhe

*Moscow State University, Institute of Nuclear Physics,
Moscow 119 899, USSR

Kernforschungszentrum Karlsruhe GmbH
Postfach 3640, 7500 Karlsruhe 1

ISSN 0303-4003

Abstract:

Elastic $^{12}C + ^{12}C$ scattering cross sections measured at incident energies of 13.8 MeV/amu and of 9.8 MeV/amu are analysed within the semimicroscopic approach of the standard double-folding model. The influence of different forms of the ^{12}C-nucleon density distribution is studied. It turns out that the experimental cross sections give some preference for a density distribution resulting from an α-cluster model description of ^{12}C.

Zusammenfassung:

KERNSTRUKTUR-EFFEKTE IN DER ELASTISCHEN $^{12}C + ^{12}C$ STREUUNG

Experimentelle Wirkungsquerschnitte für die elastische Streuung von ^{12}C an ^{12}C wurden für verschiedene Projektilenergien (13,8 MeV/Nukleon und 9,8 MeV/Nukleon) auf der Basis des Doppelfaltungsmodells analysiert. Der Einfluß verschiedener Formen der Dichteverteilung der Nukleonen in ^{12}C wurde studiert. Es stellte sich heraus, daß die Daten eine Dichteverteilung bevorzugen, die sich aus einer α-Cluster-Modell Beschreibung des Kerns ^{12}C ergibt.

1. INTRODUCTION

Elastic scattering of medium energy protons and α-particles has been extensively analysed with respect to the effective nucleon-nucleon interaction ruling microscopically the scattering process as well as to the information on the radial shape of the nuclear matter distributions of the target nuclei[1]. In contrast, though microscopic approaches have been widely used for scattering of heavier ions, in particular with the double-folding model based on realistic interactions like the M3Y interaction[2], the aspects of the reaction mechanism have been emphasized[3] rather than the structure of the underlying matter distributions. Due to the increased strong absorption in nucleus-nucleus interactions only the peripherial region appears to be sensitively probed. However, just this feature may be useful in the particular case when studying the manifestation of surface clustering of the nuclear density distributions in scattering systems like ^{6}Li + ^{6}Li, ^{6}Li + ^{12}C and ^{12}C + ^{12}C. In fact, the scattering of projectiles with pronounced cluster-structure and large break-up probabilities show some anomalies in the strengths of the real part of the optical potential which have been explained as a consequence of the continuum coupling to the break-up channels[4–6]. Alternatively, an ad hoc double-folding cluster model approach generated from d - α and α - α interactions and internal cluster wave functions of the projectile and target nuclei has been proven rather successful in the analysis of 156 MeV ^{6}Li scattering [7,8] from ^{6}Li and ^{12}C. This indicates that as far as only the nuclear surface is involved a clusterized distribution approximates the reality better than an uncorrelated single nucleon distribution.

In the present note elastic ^{12}C + ^{12}C differential cross sections, measured at E_{Lab} = 161 MeV and E_{Lab} = 117 MeV [9,10], are considered in view of the information about the nuclear periphery. The data are analysed within the framework of the standard double-folding model [2] for the real part of the optical potential

$$U_R(\mathrm{R}) = \int d\mathbf{r}_1\, d\mathbf{r}_2\, \rho_1^m(\mathbf{r}_1)\cdot\ \rho_2^m(\mathbf{r}_2)\ V(\mathbf{r}_{12} = \mathrm{R} + \mathbf{r}_2 - \mathbf{r}_1) \qquad (1)$$

using various standard effective interactions V ($\mathbf{r}_{12}$) and comparing different forms of the nucleon density distributions of ^{12}C ($\rho_1^m = \rho_2^m$), one of which is generated by a cluster model[11].The specific shapes of the nucleon density distributions affect distinctly the elastic scattering cross sections, and the cluster-model distribution prove to be slightly superior in describing the experimental data.

2. INGREDIENTS OF THE DOUBLE-FOLDING MODEL CALCULATIONS

Three different forms of the nucleon density distribution of ^{12}C are studied:

(i) the density resulting from theoretical calculations with the hyperspherical-function method (GSF)[12].

(ii) the density obtained by the 3α-resonating-group method (CL) on the basis of a cluster model[11].

(iii) the density extracted from experimental elastic electron scattering[13] data ^{12}C (e, e) ^{12}C (EL).

The method of hyperspherical functions expresses the nuclear wave functions by an expansion in hyperspherical harmonics [12]

$$\Psi = \sum_K \chi_K(\rho)\, Y_{K\nu}(\theta) \tag{2}$$

which are eigenfunctions of the angular part Δ_{Ω_n} of the Laplacian

$$\Delta_{\Omega_n} Y_{K\nu}(\theta_i) = -K(K+n-2)\, Y_{K\nu}(\theta_i) \quad . \tag{3}$$

The hyperspherical coordinates (angles Θ_i and radius ρ) are related to the normalized Jacobi coordinates (see ref. 12). The diagonal ($i = j$) and transition ($i \neq j$) densities are given by

$$\rho_{ij}^{m}(r) = \frac{16}{\sqrt{\pi}} \frac{\Gamma\left(\frac{5A-11}{2}\right)}{\Gamma\left(\frac{5A-14}{2}\right)} \int_r^\infty \frac{(\rho^2 - r^2)^{\frac{5A-16}{2}}}{\rho^{5A-13}} \chi_i(\rho)\chi_j(\rho)\, d\rho +$$

$$\frac{8}{3} \frac{(A-4)}{\sqrt{\pi}} \frac{\Gamma\left(\frac{5A-11}{2}\right)}{\Gamma\left(\frac{5A-16}{2}\right)} \int_r^\infty \frac{r^2(\rho^2 - r^2)^{\frac{5A-18}{2}}}{\rho^{5A-13}} \chi_i(\rho)\chi_j(\rho)\, d\rho \tag{4}$$

The cluster model densities (CL) calculated with the 3α-resonating group method by Kamimura[11] are parametrized in the form

$$\rho_{ij}^{m(\lambda)} = \sum_{s=1}^{N} C_{ij}^{\lambda}(s)\,(r/r_s)^{\lambda}\, exp\,(-r^2/r_s^2) \tag{5}$$

with parameters given in ref. 11.

When adopting a density distribution of ^{12}C extracted from elastic electron scattering (EL), a three parameter Fermi distribution[13]

$$\rho^{m}(r) = \rho_o(1 + w r^2/c^2)/(1 + exp[(r-c)/z]) \tag{6}$$

with $\quad c = 2.355$ fm $\quad w = -0.149 \quad z = 0.5224$

is used.

The three different forms of the ground-state density of ^{12}C exhibit considerable differences. However due to the strong absorption of the ^{12}C + ^{12}C interaction only the tails determine dominantly the ^{12}C scattering. Actually, they are less sensitively probed in the outermost region by electron scattering[1].

The real part of the optical potential is generated by eq. (1) with the M3Y (density independent) and DDMY3 (density dependent) energy dependent effective nucleon-nucleon interactions as specified by El-Azab Farid and Sachtler[14]

$$V(E,\rho^m,s) = g(E,s)\, f(E,\rho^m) \tag{7}$$

where

$$f(E,\rho^m) = C(E)[1 + \alpha(E)e^{-\beta(E)\rho^m}] \tag{8}$$

and g(E,s) is the original M3Y interaction whose spin- and isospin-independent part is given in MeV by

$$g(E,s) = [7999e^{-4s}/4s - 2134e^{-2.5s}/2.5s] + \hat{J}(E)\delta(s) \quad . \tag{9}$$

Here, E is the bombarding energy per nucleon, s = r_{12} is the internucleon separation, and ρ^m is the density of nuclear matter in which the interacting nucleons are embedded. We take $\rho^m = \rho_1^m(r_1) + \rho_2^m(r_2)$ for a nucleon at r_1 in nucleus 1 interacting with a nucleon at r_2 in nucleus 2 (sudden approximation [15,16]) since mainly the nuclear surface is involved. The term $\hat{J}(E)$ represents the effect of knock-on exchange between the interacting nucleons with

$$\hat{J}(E) = -276(1 - 0.005E) \quad (MeV \cdot fm^3) \quad . \tag{10}$$

The parameters of the density dependent factor (eq. 8) are adopted from ref. 14.

When calculating the cross sections on the basis of the folding model it is generally found that the interaction strength U_R has to be renormalized by an overall factor N (around 1) in order to fit the experimental data. This factor N has been adjusted together with the parameters W, r_W and a_W of a phenomenological Woods-Saxon form of the imaginary part of the optical potential, applying a χ^2 - minimization procedure. Values of N $\approx$ 1.0 indicate success of the model while any deviation of N from unity implies deficiencies of the model calculations. A charge radius parameter r_c = 1.05 fm was used for the Coulomb potential.

3. RESULTS

Figure 1 displays the real part of the optical potential resulting from different procedures and corresponding to the adjusted theoretical cross sections shown in Figs 2 and 3.

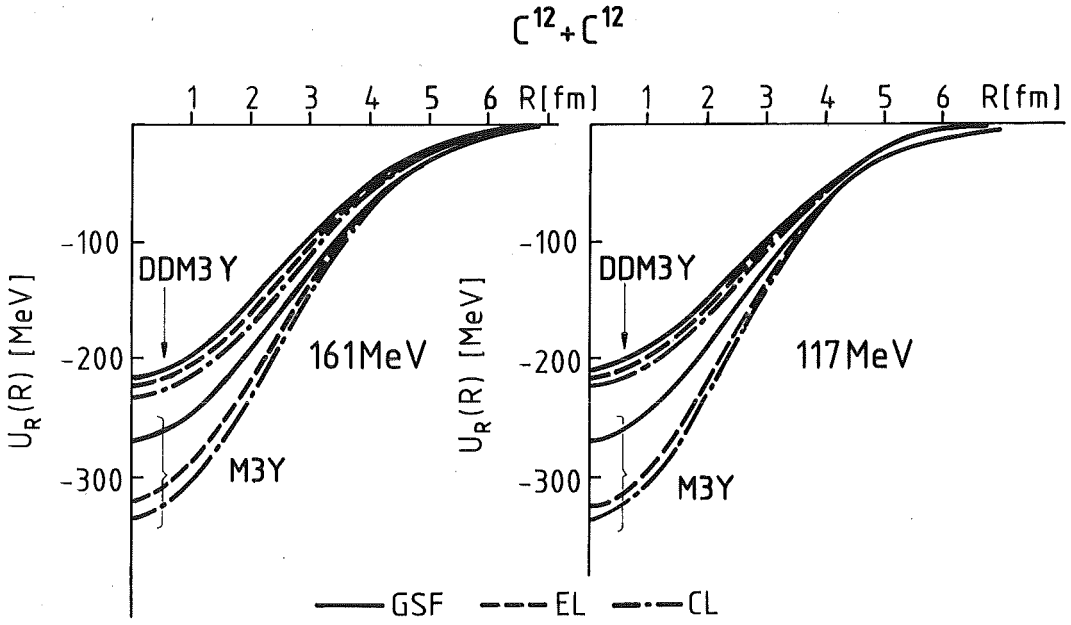

Fig. 1 Real part U_R of the ^{12}C + ^{12}C optical potentials calculated with the M3Y and DDM3Y nucleon-nucleon forces for different forms of the density distribution ρ^m.

We see the well known differences[2,14] in depths of the DDM3Y and M3Y potentials, in particular at small radii. The dependence on the specific form of the density distribution alters the shape of the potential at larger radii beyond the strong absorption radius and leads to differences in the calculated cross sections.

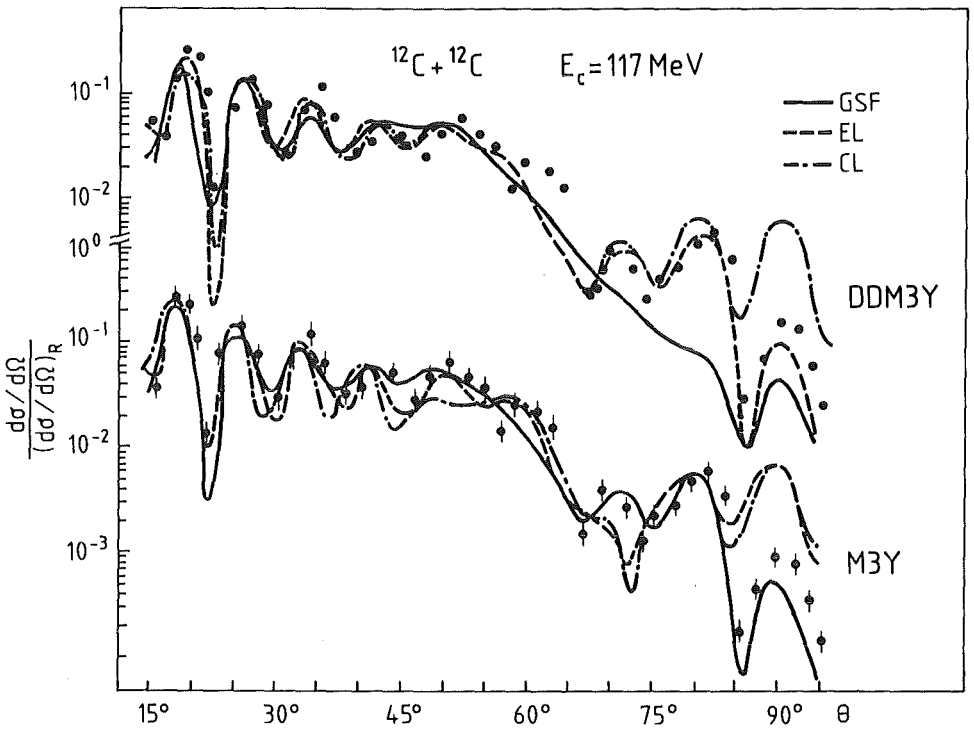

Fig. 2 Elastic scattering of 117 MeV ^{12}C from ^{12}C as compared with the folding model calculations.

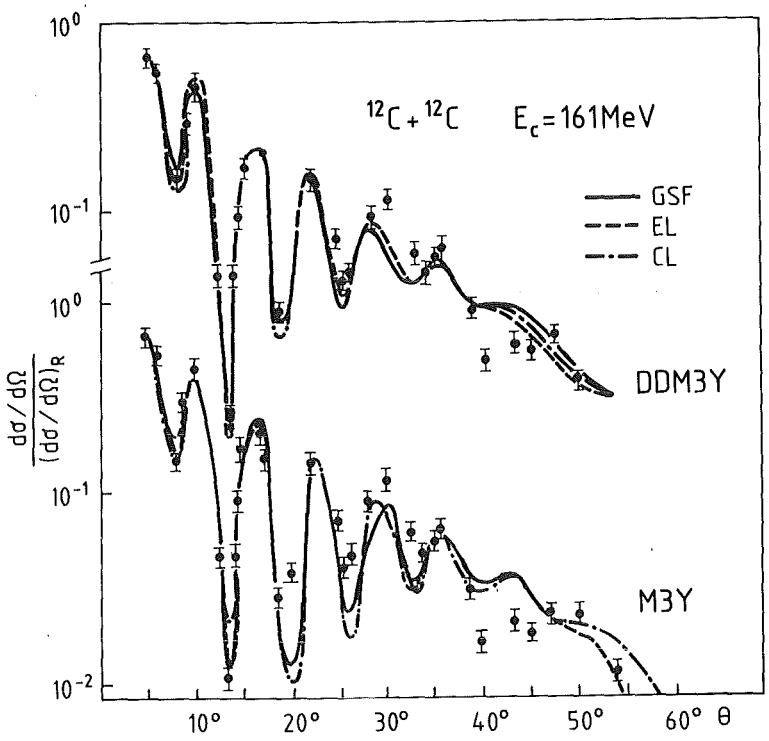

Fig. 3 Experimental and theoretical differential cross sections for 161 MeV ^{12}C + ^{12}C elastic scattering.

Tab. 1 Best fit parameters and results of the double-folding model analysis of elastic $^{12}C + ^{12}C$ scattering.

E_{Lab} [MeV]	ρ^m	Interaction	N	W [MeV]	r_w [fm]	a_w [fm]	χ^2/F	σ_R [mb]	J_w [MeV·fm^3]
161.1	GSF	M3Y	0.64	55.0*	0.91*	0.80*	10.3	1512	1894.5
			0.66	133.5	0.86	0.65	7.2	1419	3673.8
		DDM3Y	0.53	46.2	0.91	0.80	8.8	1457	1591.0
	CL	M3Y	0.84	55.0*	0.91*	0.80*	23.6	1505	1812.2
			0.907	133.6	0.84	0.68	20.8	1430	3402.9
		DDM3Y	0.82	60.5	0.91	0.77	9.9	1477	1993.7
	EL	M3Y	0.79	55.0*	0.91*	0.80*	13.9	1507	1934.3
			0.847	141.9	0.84	0.68	11.2	1427	3407.0
		DDM3Y	0.714	55.2	0.93	0.74	7.4	1412	1942.4
117.0	GSF	M3Y	0.67	16.0	1.19	0.63	19.1	1425	1025.6
		DDM3Y	0.536	11.7	1.25	0.63	37.6	1438	850.0
	CL	M3Y	1.01	17.4	1.21	0.64	23.3	1477	1153.5
		DDM3Y	0.82	14.7	1.21	0.63	18.4	1420	973.0
	EL	M3Y	0.813	16.3	1.20	0.62	16.0	1440	1050.2
		DDM3Y	0.835	15.5	1.22	0.61	26.50	1440	1050.0

* Parameter of the imaginary part taken from ref. 10

Table 1 compiles the parameter values of the optical potentials resulting from the fitting procedure. We feel that the values of the volume integral J_W are not very significant as surface absorption is dominant. The values of the reaction cross section σ_R agree fairly well with results of other analyses (see ref. 10) and direct measurements[17]. Though we have to admit that details of the experimental cross sections (for which a better determination of the oscillation pattern by additional data points in the forward hemisphere would have been helpful) are less well reproduced than by a phenomenological optical model analysis[9], we see some preference for the cluster-model density distribution, in particular through the fact that the renormalization factor N approaches best the unity in that case.

4. CONCLUDING REMARKS

Recently[18] the polarization potential arising from the excitation and from 3α-break-up of ^{12}C has been calculated and added to a microscopically derived optical potential which is shown to overestimate the elastic scattering cross section of ^{12}C + ^{12}C scattering at 30 MeV/amu. This successful procedure improves the agreement with the data and is just in the spirit of the coupled discretized continuum channels approach of Kamimura et al.[5] which remedies the deficiency of folding model calculations requiring N significantly smaller than unity in presence of strong projectile break-up contributions.

As already concluded from previous analyses of ^{6}Li scattering[7,8] the present results indicate that an adequate inclusion of clusterization in the density distribution of the scattered nuclei may provide an alternative procedure to account for the effect.

REFERENCES

1. C.J. Batty, E. Friedman, H.J. Gils and H. Rebel, Advances in Nuclear Physics, Vol. **19**, eds. J.W. Negele and E. Vogt, Plenum Press, New York (1989)
2. G.R. Satchler and W.G. Love, Phys. Rep. **55** (1979) 183
3. K.V. Shitikova, Part. Nuclei **16** (1985) 824
4. I.J. Thompson and M.A. Nagarajan, Phys. Lett. **106** B (1981) 163
5. Y, Sakuragi, M. Yahiro, M. Kamimura, Prog. Theoret. Phys. **70** (1983) 1047
6. Y. Sakuragi, M. Kamimura, S. Micek, H. Rebel and H.J. Gils, Z. Phys. **A322** (1985) 627

7. Z. Majka, H.J. Gils and H. Rebel, Phys. Rev. **C25** (1982) 2996

8. S. Micek, Z. Majka, H. Rebel, H.J. Gils and H. Klewe-Nebenius, Nucl. Phys. **A435** (1985) 621

9. A.J. Cole, W.D.M. Rae, M.E. Brandan, A. Dacal, B.G. Harvey, R. Legrain, M.J. Murphy and R.G. Stokstad, Phys. Rev. Lett. **47** (1981) 1705
R.G. Stokstad, R.M. Wieland, G.R. Satchler, C.B. Fulmer, D.C. Hensley, S. Raman, L.D. Rickertsen, A.H. Snell and P.H. Stelson, Phys. Rev. **C20** (1979) 655

10. M.E. Brandan, J. Phys.: Nucl. Phys. **9** (1983)

11. M. Kamimura, Nucl. Phys. **A351** (1981) 456

12. K.V. Shitikova, Nucl. Phys. **A331** (1979) 365

13. C.W. de Jager, H. de Vries and C. de Vries, Atomic Data and Nuclear Data Tables 14 (1974) 479

14. M. El-Azab Farid and G.R. Satchler, Nucl. Phys. **A438** (1985) 525

15. Z. Majka, H.J. Gils and H. Rebel, Z. Phys. **A288** (1978) 1220

16. H.J. Gils, Nucl. Phys. **A473** (1987) 111

17. R. Cherkaoui-Tadili, Thesis Université Scientifique et Médicale de Grenoble (1982)

18. G. Pantis, R. Linden, N. Ohtsuka and Amand Faessler, preprint Universität Tübingen (1989)